Augusteyn, Robert C. and Jones, Catherine E. and Pope, James M. (2008) ***Age-related development of a refractive index plateau in the human lens : evidence for a distinct nucleus.*** Clinical and Experimental Optometry, 91(3). pp. 296-301.

Age-related development of a refractive index plateau in the human lens: evidence for a distinct nucleus

Robert C Augusteyn[1,2], Catherine E Jones[3*] and James M Pope[3,4]

1. Institute for Eye Research, Sydney, Australia

2. Ophthalmology Department, University of Melbourne, Melbourne, Australia

3. School of Physical & Chemical Sciences, Queensland University of Technology, Brisbane, Australia

4. Institute for Health and Biomedical Innovation, Queensland University of Technology, Brisbane, Australia

*Current address: Department of Radiology, University of Pennsylvania, Philadelphia, USA.

Corresponding Author:

Robert C. Augusteyn Ph.D.

Vision CRC

30 Melcombe Rd

Ivanhoe Vic 3079

Australia

Email: raugustn@bigpond.net.au

Telephone: +61 3 9499 1838

Key words: lens, growth, nucleus, refraction, gradient, RI plateau

Abstract

The human lens comprises two distinct regions in which the refractive index changes at different rates. The outer 1.09 mm contains a rapidly increasing refractive index gradient, which becomes steeper with age. The inner region contains a shallow gradient which flattens with age due to formation of a central plateau, of RI = 1.418, which reaches a maximum size of 7.0 x 3.05 mm around age 60. Formation of the plateau can be attributed to compression of fibre cells generated in prenatal life. γ-crystallin, present in prenatal but not in postnatal fibre cells, may play a role in limiting nuclear cell compression.

Introduction

The lens grows throughout life, slowing with increasing age. As it does, mature fibre cells are compressed into the central or nuclear region, losing water and organelles in the process. Since there is no breakdown of proteins, their concentration in the cell, and hence the refractive index, increases. This process results in the generation of a refractive index gradient, essential for reducing spherical aberration.

Early studies by Pierscionek and Augusteyn,[1] using the elegant laser ray tracing technique developed by Campbell and Hughes,[2] and modified by Pierscionek, Chan, Ennis, Smith and Augusteyn[3] indicated that the shape of the refractive index gradient (GRIN) varies with species. They showed that rat and fish lenses have a steep and continuous gradient ranging from about 1.39 at the periphery to as high as 1.55 in the centre. More recently, Garner, Smith, Yao and Augusteyn,[4] using a magnetic resonance imaging (MRI) technique developed by Moffatt and Pope[5,6] and described in detail by Moffat, Atchison and Pope,[7] as well as laser ray tracing, noted the same shaped gradient in the Black Oreo Dory. Coupled with the spherical shape, such lenses provide an animal with the high power required for very close vision. However, this is at the cost of flexibility since these lenses are extremely hard. By contrast, mammalian lenses were found to have a relatively shallow gradient with a maximum refractive index (RI) under 1.45.[1] Combined with elliptical surfaces, these lenses have a lower power. They are softer and their shape can be altered to provide different focal lengths in species capable of accommodation.

In most lenses studied, the refractive index at the centre increases with age. However, the human lens is different. Even though growth and compression continue throughout life,[8] the RI does not increase beyond about 1.415 and appears to plateau in the centre of the lens.[1] A similar conclusion can be reached from the distribution of protein determined by Fagerholm, Philipson and Lindstrom,[9] using microdensitometry and from the Raman microspectroscopic observations of Siebinga, Vrensen, de Mul and Greve[10].

The shape of the RI gradient and the presence of a plateau region in old human lenses were confirmed in a recent study by Jones, Atchison, Meder and and Pope,[11] using MRI. They noted that with increasing age, the refractive index profile became flatter in the centre of the lens while at the periphery it became steeper. No attempt was made to examine the size of the plateau or the rate at which it developed.

Deleted: a

In the current communication, the MRI data from 20 lenses, aged from 7-82 years, were used to examine the development of the RI plateau. The analyses indicate that a plateau of constant RI gradually develops with age and reaches a maximum width around age 60.

Materials and Methods

Refractive index gradients along both axial (sagittal) and equatorial directions in the lens were obtained from the magnetic resonance imaging study on 20 human lenses, aged 7-82 years, described previously by Jones et al.[11]

Each point in the RI profile data was subjected to one round of smoothing, by averaging it with the point before and the point after, and then the incremental changes in RI were calculated in order to determine the gradient in refractive index (GRIN) for both the equatorial and sagittal axes. Regression analysis was used to determine the slope of the refractive index gradient in the outer 1 mm and in the central region. In a few cases, this was not possible because of large scatter in the RI values, possibly due to localised artefacts or interference in the raw MR images from which the values were obtained. The sections of the central regions in which the RI gradient was below 0.0001/mm and for which the SD of the average RI was less than 0.2%, were considered to represent the plateau region in the lens.

Protein concentrations were calculated using the refractive increments of the crystallins[12] and their proportions in different parts of the lens.[13]

Results

Typical RI profiles, from 7, 55 and 82 year old lenses, are presented in Figure 1. Inspection of these reveals, as noted by Jones et al,[11] that the RI gradient at the outside of the lens becomes steeper with age and the RI profile in the central region becomes flatter. It would appear that the flattening of the profile is due to the outward spread of the RI maximum (1.418 ± 0.0075).

In order to characterize these age-dependent changes, the refractive index gradient was calculated for each lens as a function of position along the sagittal and equatorial directions. Typical plots, for the 7 yo and 82 yo lenses shown in Fig 1, are presented in Figure 2 and 3 respectively. The plots reveal that, particularly for the older lenses, the refractive index profiles consist of two regions where the RI changes at different rates, rapidly in the outer parts of the lens and slowly in the centre.

Figure 4 plots the rates of change of the refractive index gradient (i.e. the slopes of plots such as Figures 2 and 3) in the outer 1mm of the lenses as a function of lens age. The slope of the RI gradient in the outer equatorial region has a value of around 0.08/mm^2 for both sides of the lens at all ages (Figure 4a). For the sagittal axis, the anterior slope was greater than that of the posterior slope and both increased with age from around 0.1/mm^2 and 0.09/mm^{2}at age 7, (for the anterior and posterior slopes, respectively), to around 0.13/mm^2 and 0.11/mm^2 at age 82 (Figure 4b).

The RI gradient changes much more slowly in the middle of the lens but the changes are more complex. In the 7 yo lenses, the RI gradient changes at 0.005/mm^2 (R^2 = 0.90) along both the equatorial and sagittal directions. However, in the older lenses, the shape of the RI profile changes due to the formation of a short section in the centre where the slope becomes zero, i.e. a plateau in the refractive index.

A schematic representation of the changes in RI gradient through a typical lens is shown in Figure 5. The points comprising the plateau and the corresponding line of best fit are shown in blue in Figures 2 and 3. In the 7 yo old lens (Figure 2), the plateau is difficult to see, especially along the equatorial direction, but it becomes obvious in older lenses. The width of the plateau increases with age so that, in the 82 yo lens, it appears to occupy the whole of the central region (Figure 3).

Under ideal conditions, in plots of refractive index gradient such as Figures 2 and 3, a plateau region should have both a slope and an intercept of zero. Therefore, linear regression was used to identify regions in the central profile where the change in GRIN slope was less than $0.001/mm^2$ and/or the extrapolated incremental intercept was 0.0 ± 0.001. The estimated plateau widths in the sagittal and equatorial axis are presented in Figure 6. The data suggest that the sagittal plateau appears earlier and develops more quickly than that in the equatorial axis. Both plateaus appear to have reached their maximum widths, $3.05 \pm .09$ and 7.0 ± 0.03 mm, by about age 60.

Discussion

Our calculations from the MRI data of Jones et al[11] indicate that there are two distinct regions in the lens, which appear to change independently with age, an outer region of rapidly changing RI gradient and a central region of very slow change. The identification of these two regions is consistent with the recent report that human lens growth is biphasic, with most of the central or nuclear region being generated prenatally in a self-limiting process, and the outer tissue generated postnatally through linear growth.[8]

Deleted:

The outer region contains a steep gradient of refractive index, which along the sagittal axis gradually becomes steeper with increasing age, more noticeably in the anterior of the lens. There appears to be no age-related change along the equatorial direction. By contrast, the RI in the central region changes very slowly along both axes and the gradient gradually decreases with age due to the formation of a central plateau at a refractive index of 1.418. In the youngest lenses examined (7 year old) the plateau is very small but it is clearly evident in older lenses and, with increasing age, there is a gradual increase in its width in both sagittal and equatorial directions until about age 60. Thereafter, no further increases were observed even though the lens continues to increase in size.

The maximum dimensions of the constant RI region (7.0 x 3.05 mm) are very similar to the dimensions of the hydrodissected nucleus (7x3 mm)[14] and to the location of the diffusion barrier (7.2x2.8 mm from the centre)[15] The small differences can probably be attributed to differences in the hydration state of the lenses as a result of storage.[16] In addition, it would appear that the plateau boundary is close to the location of the first zone of discontinuity in >40 yo lenses. According to Koretz, Cook and Kuszak,[17] the inner edge of Zone 1 in the anterior cortex of a fully accommodated lens, in vivo, lies at 1.094 ± .085 mm from the sulcus. This corresponds to 63% of the anterior sagittal thickness and may be compared with the 60% of total sagittal thickness occupied by the plateau region.

These similarities lead to the conclusion that the plateau region arises from the lens material laid down in prenatal life, i.e. the combined foetal and embryonic nuclei. These were generated during the prenatal asymptotic growth mode. The tissue on the outside, containing most of the refractive index gradient, is generated postnatally in the linear growth mode, which continues throughout the rest of life.[8] The observations of Taylor, Al-Ghoul, Lane, Davis, Kuszak, and Costello,[18] that the cells in the foetal and embryonic nuclei were larger and more rounded than those in the juvenile and adult nuclei and cortex, are consistent with the conclusion that the two sets of tissue are produced through different growth modes and have different properties.

Lyophilization of old whole human lenses yields an intact nucleus, weighing 30-33 mg while the remaining tissue disintegrates.[19] This observation implies that the inner and outer regions of the lens have different properties and are not strongly connected. The splitting of the two regions probably occurs in the area containing the diffusion barrier. It may be calculated, using the RI increments determined by Pierscionek, Smith and Augusteyn,[12] that the constant RI tissue in >60 yo lenses contains around 31 mg of protein. This is very close to the observed weights of the lyophillized nuclei and also corresponds closely to the mass of protein produced during the prenatal logarithmic growth phase (Augusteyn, unpublished). These observations add further support to the suggestion that the plateau region in the lens corresponds to a distinct structural entity produced from cells laid down during a prenatal growth phase, which is different from that generating the refractive index gradient in postnatal life.

With continued postnatal lens growth, the prenatal cells are packed into the centre of the lens and compressed until they reach the constant maximum RI of 1.418. Our data indicate that maximum compression is reached first in the centre and then spreads outwards. Thus, it would be expected that fibre cell sizes would vary with position in the lens. According to Al-Ghoul et al,[20] embryonic and foetal fibre cells are compressed by an average of about 30% in old (59-81 years) lenses when compared with 15-25 yo lenses. Much of this compression is already evident in lenses aged 36-46 years where both primary and secondary fibre cells average around 79% of their size in 15-25 yo lenses. However, significant compression has taken place prior to birth (Augusteyn, unpublished) suggesting that the above estimates may be low.

The changes in protein concentration are also consistent with substantial fibre cell compression. The RI at the outside corresponds to a protein concentration of 17% (w/v). At the intersection of the fast and slow RI change regions in the 7 yo lens, it is around 24% and in the centre of the oldest lenses, it is 38%. Since there is no protein turnover in the mature fibre cells, these concentrations suggest that fibre cells are compressed to around 60 % of their original volume. However, it should be noted that the outer region of the lens contains immature fibre cells, which may not yet have produced their full, final complement of proteins.

The extent of compression may be determined, in part, by the properties and proportions of the proteins in the cells, in particular, the β- and γ-crystallins. Interactions between γ-crystallins are attractive so that they are capable of self- association.[21] This decreases their requirement for interaction with water, through reductions in their hydration shells and osmolality. However, the interactions between the β-crystallins are repulsive. These observations suggest that γ-crystallin promotes the loss of water from a lens cell while β-crystallin promotes water retention. In the human lens, α-crystallin represents a constant proportion of the lens proteins at all stages of life. β- and γ-crystallins make up most of the remainder but their relative amounts vary with age. γ-crystallin synthesis takes place only in the prenatal lens where it represents a constant proportion of the total proteins.[13] Its synthesis ceases at, or immediately after birth so that only the nuclear region of the human lens contains γ-crystallins. Thus, it might be envisaged that the loss of water from the prenatal tissues is driven by the concentration of γ-crystallin present. It is interesting to note that rodent lenses, which have higher γ-crystallin contents and in which the protein is synthesized throughout life, lose much more water resulting in higher refractive index levels and harder tissues. On the other hand, bird and reptile lenses, which contain no γ-crystallin, do not appear to compress at all (RC Augusteyn, unpublished).

The RI profiles and the incremental plots contain a number of small bumps, many of which appear to be present in most lenses, examined. A small central dip probably represents the sulcus. However, the noise in the data prevented unequivocal assignment of their locations. The data used in this study were acquired at a magnetic field strength of 4.7 Tesla. It would be of great interest to examine these features, as well as lenses from other species, using higher field MRI systems capable of improved resolution and signal to noise (S/N) ratio.

Acknowledgements

This work was supported by NIH consortium grant RO1EYO14225, the Cooperative Research Centre Scheme of Australia and Queensland University of Technology.

References

1. Pierscionek BK, Augusteyn RC. Species variability in optical parameters of the eye lens. Clin Exp Optom1993; 76: 22-25.

2. Campbell MCW, Hughes AA. An analytic gradient index schematic lens and eye for the rat which predicts aberrations for finite pupils. Vis Res 1981; 21: 129-1148.

3. Pierscionek BK, Chan C, Ennis JP, Smith G, Augusteyn RC. Nondestructive method of constructing three-dimensional gradient index models for crystalline lenses: I. Theory and experiment. Am J Optom Physiol Optics1988; 65: 481-491.

4. Garner LF, Smith G, Yao S, Augusteyn RC. Gradient refractive index of the crystalline lens of the Black Oreo Dory (Allocyttes Niger): comparison of magnetic resonance imaging (MRI) and laser ray-trace methods. Vis Res 2001; 41: 973-979.

5. Moffatt BA, Pope JM. Mapping of refractive index distribution in crystalline lenses using transverse relaxation (T_2) imaging. Proc. 5th Int Conf Magn Reson Micros 1999; 28: (Abstract).

6. Moffatt BA, Pope JM. Mapping of refractive index distribution in crystalline lenses using transverse relaxation (T_2) imaging. Proc. 3rd Biennial Conf. ANZ Soc Magn Reson 2000, 101 (Abstract).

7. Moffatt BA, Atchison D., Pope JM. Age-related changes in refractive index distribution and power of the human lens as measured by magnetic resonance micro-imaging in vitro. Vis Res 2002; 42: 1683-1693.

8. Augusteyn RC. Growth of the human lens. Mol Vis 2007; 13: 252-257.

9. Fagerholm PP, Philipson BT, Lindstrom R. Normal human lens, the distribution of protein. Exp Eye Res 1981; 33: 615-620.

10. Siebinga I, Vrensen GJM, de Mul FFM, Greve J. Age-related changes in local water and protein content of human eye lenses measured by Raman microspectroscopy. Exp Eye Res 1991; 53: 233-239.

11. Jones C, Atchison DA, Meder R, Pope JM. Refractive index distribution and optical properties of the isolated human lens measured using magnetic resonance imaging (MRI). Vis Res 2005; 45: 2352-2366.

12. Pierscionek B Smith G, Augusteyn RC. The refractive increments of bovine α-, ß- and γ-crystallins. Vis Res 1987; 27: 1539-1541.

13. Thomson JA, Augusteyn RC. Ontogeny of human lens crystallins. Exp Eye Res 1985; 40: 393-410.

14. Gullapalli VK, Murthy PR, Murthy KR. Colour of the nucleus as a marker of hardness diameter and central thickness. Ind J Ophthalmol 1995; 44:181-4.

15. Sweeney MHJ, Truscott RJW. An impediment to glutathione diffusion in older normal human lenses: a possible precondition for nuclear cataract. Exp Eye Res 1998; 67: 587-595.

16. Augusteyn RC, Rosen AM, Borja D, Ziebarth NM, Parel JM. Biometry of Primate Lenses during Immersion in Preservation Media. Mol Vis 2006; 12: 740-747.

17. Koretz JF, Cook CA., Kuszak JT. The zones of discontinuity in the human lens: development and distribution with age. Vis Res 1994; 34: 2955-2962.

18. Taylor L, Al-Ghoul KJ, Lane CW, Davis VA, Kuszak JR, Costello MJ. Morphology of the normal human lens. Invest Ophthalmol Vis Sci 1996; 37: 1396-1410.

19. Truscott RJW, Augusteyn RC. Changes in human lens proteins during nuclear cataract formation. Exp Eye Res 1977; 24, 159-170.

20. Al-Ghoul KJ, Nordgren R, Kuszak AJ, Freel CD, Costello MJ, Kuszak JR. Structural evidence of human nuclear fibre compaction as a function of ageing and cataractogenesis. Exp Eye Res 2001; 72: 199-214.

21. Tardieu A, Veretout F, Krop B, Slingsby C. Protein interactions in the calf lens; interactions between beta-crystallins are repulsive whereas in gamma-crystallins they are attractive. Eur Biophys J 1992; 21: 1-12.

Legends to figures

Figure 1 Refractive index profiles in 7 (•), 27 (•) and 82 (•) yo human lenses along a) the equatorial direction and b) the sagittal axis. The posterior sagittal edge is on the left.

Deleted: axis

Figure 2. Refractive index gradient as a function of position for the 7 yo lens, shown in Fig 1, along a) the equatorial and b) the sagittal axis. The central plateau region is indicated with solid circles (•) and the line of best fit (———).

Figure 3. Refractive index gradient as a function of position for the 82 yo lens, shown in Fig 1, along a) the equatorial and b) the sagittal axis. The central plateau region is indicated with solid circles (•) and the line of best fit (———).

Figure 4. Slope of the refractive index gradient, as a function of age, in the outer 1 mm of a) the equatorial direction (2 possible values for each lens) and b) the (•), anterior (•) and posterior sagittal axes.

Deleted: axis

Figure 5. Diagrammatic representation of the incremental RI changes across the equatorial direction, showing the outer 0-1.0 mm with slope ~ $0.07/mm^2$ (———) and the emerging plateau with zero slope (———).

Deleted: axis

Figure 6. Changes in the width of the putative plateau region (•), as a function of age, in the centre of a) the equatorial and b) the sagittal axis. The dimensions of the whole lens (•) are included in each figure for comparison.

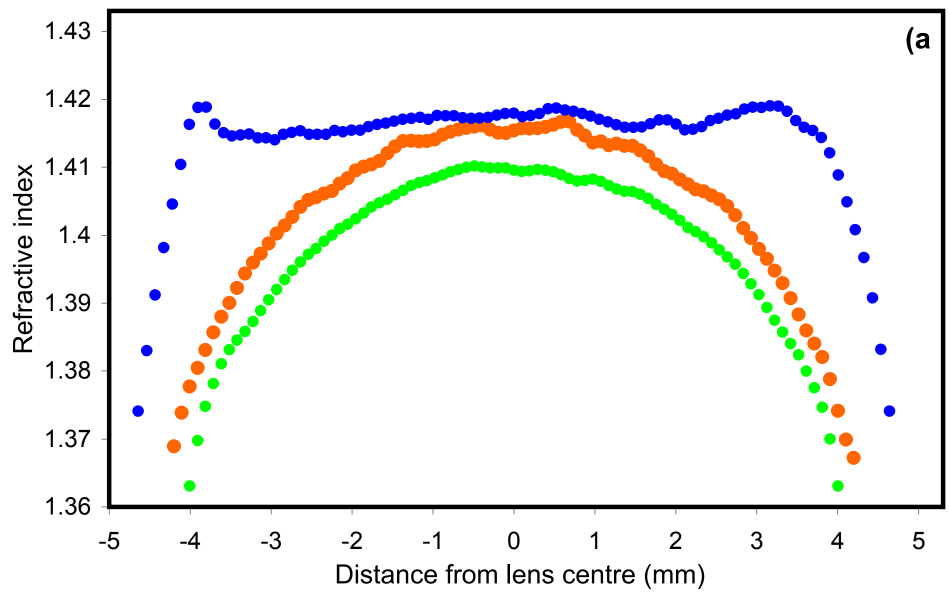
(a
1.43
1.42
1.41
1.4
1.39
1.38
1.37
1.36
Refractive index
-5
-4
-3
-2
-1
0
1
2
3
4
5
Distance from lens centre (mm)

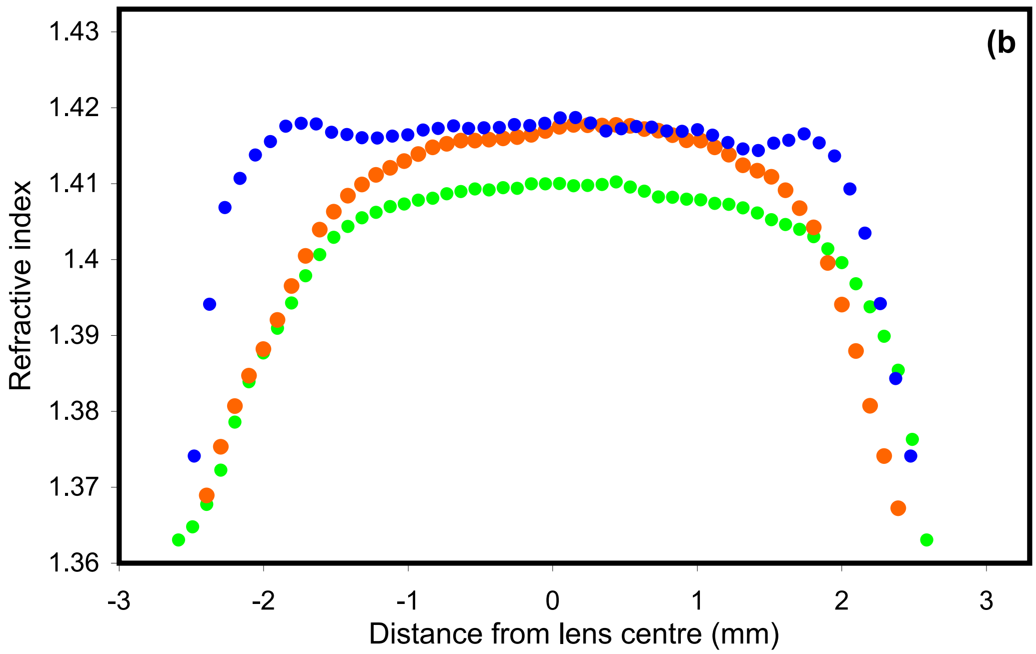
(b
Refractive index
1.43
1.42
1.41
1.4
1.39
1.38
1.37
1.36
-3
-2
-1
0
1
2
3
Distance from lens centre (mm)

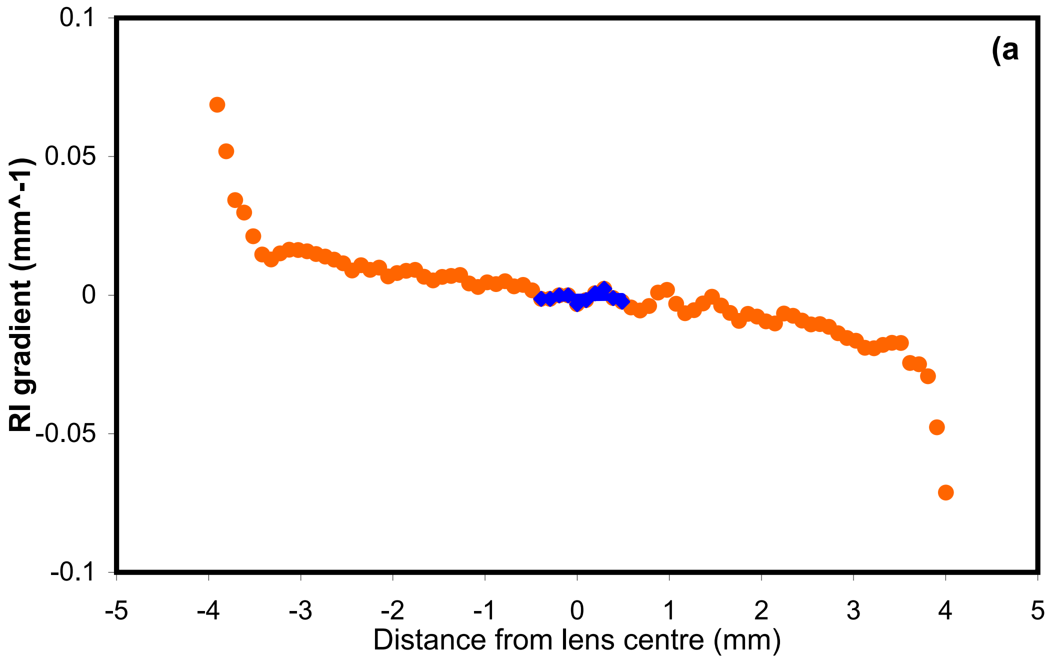
(a
RI gradient (mm^-1)
0.1
0.05
0
-0.05
-0.1
-5
-4
-3
-2
-1
0
1
2
3
4
5
Distance from lens centre (mm)

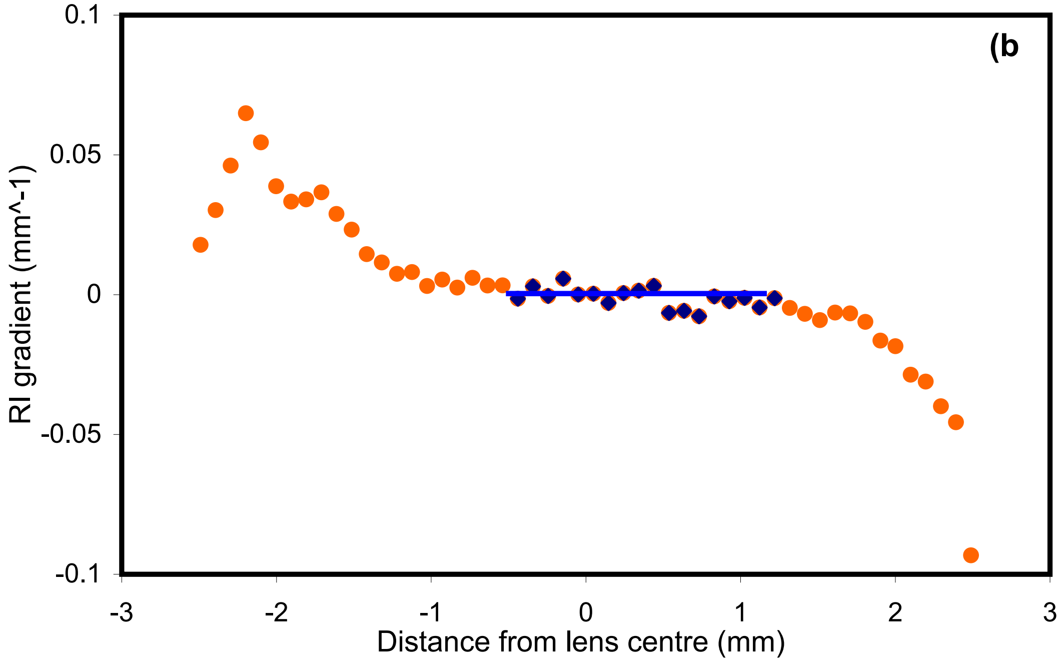
(b
RI gradient (mm^-1)
0.1
0.05
0
-0.05
-0.1
-3
-2
-1
0
1
2
3
Distance from lens centre (mm)

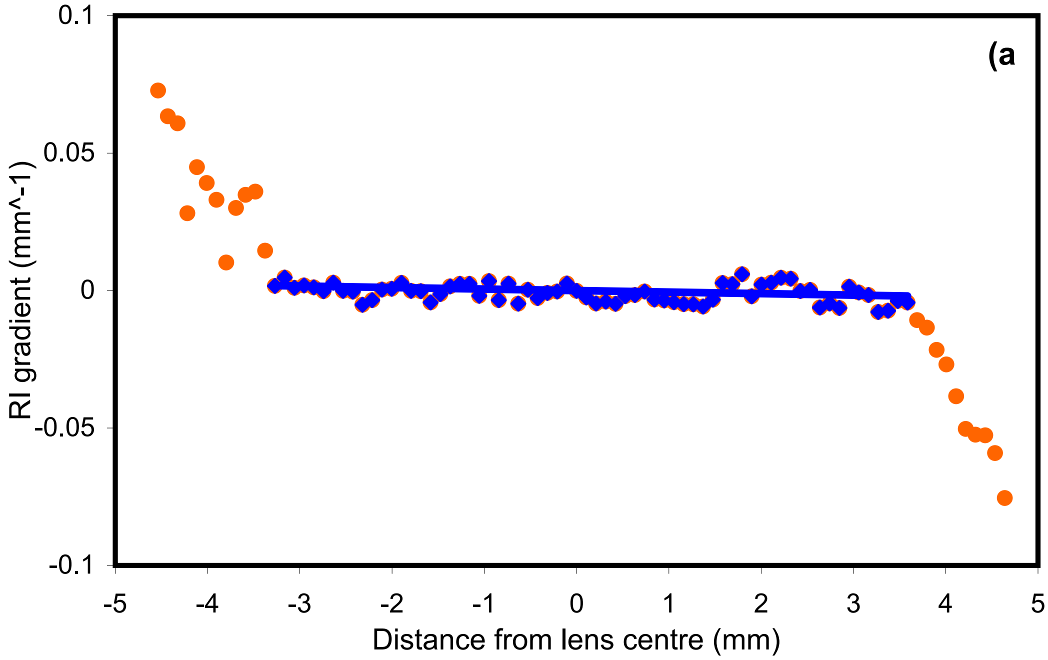
0.1
0.05
0
-0.05
-0.1
RI gradient (mm^-1)
(a
-5
-4
-3
-2
-1
0
1
2
3
4
5
Distance from lens centre (mm)

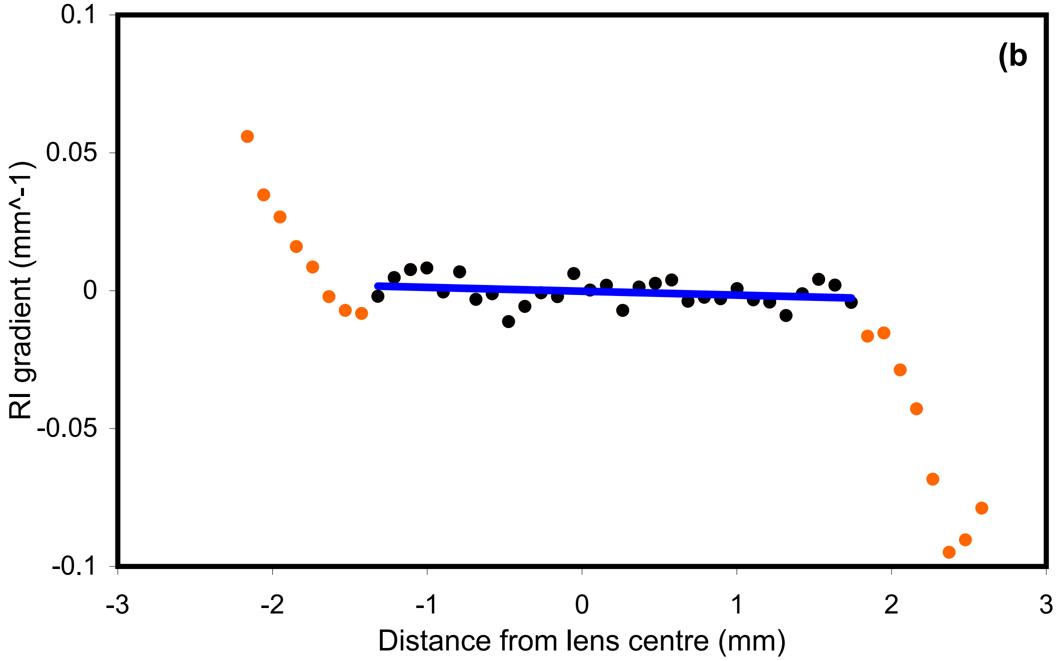

(b
RI gradient (mm^-1)
0.1
0.05
0
-0.05
-0.1
-3
-2
-1
0
1
2
3
Distance from lens centre (mm)

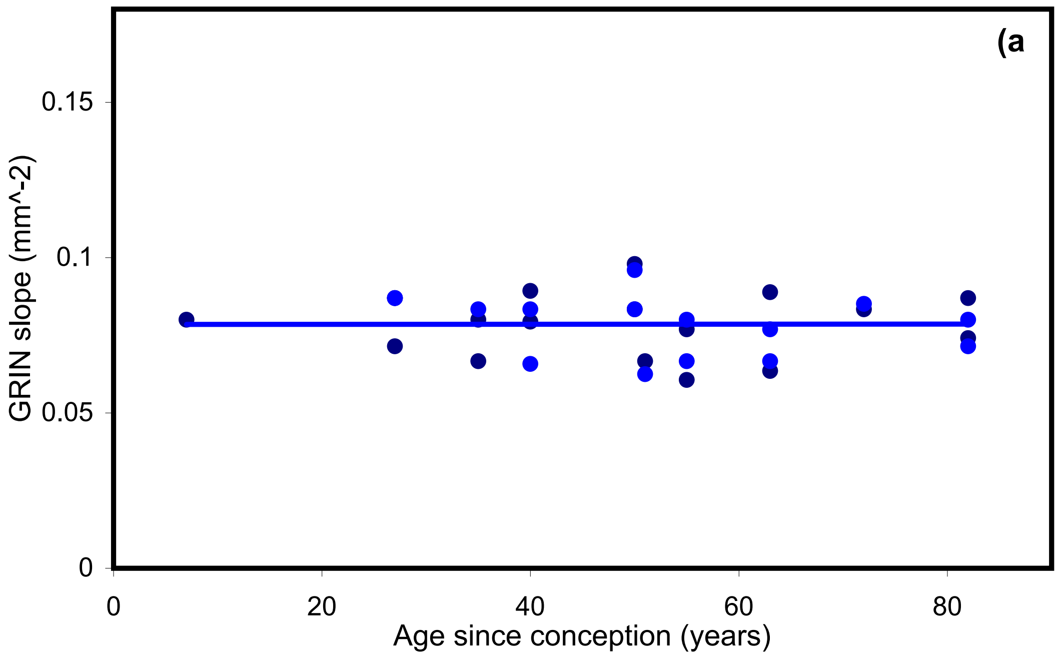
(a
GRIN slope (mm^-2)
0.15
0.1
0.05
0
0
20
40
60
80
Age since conception (years)

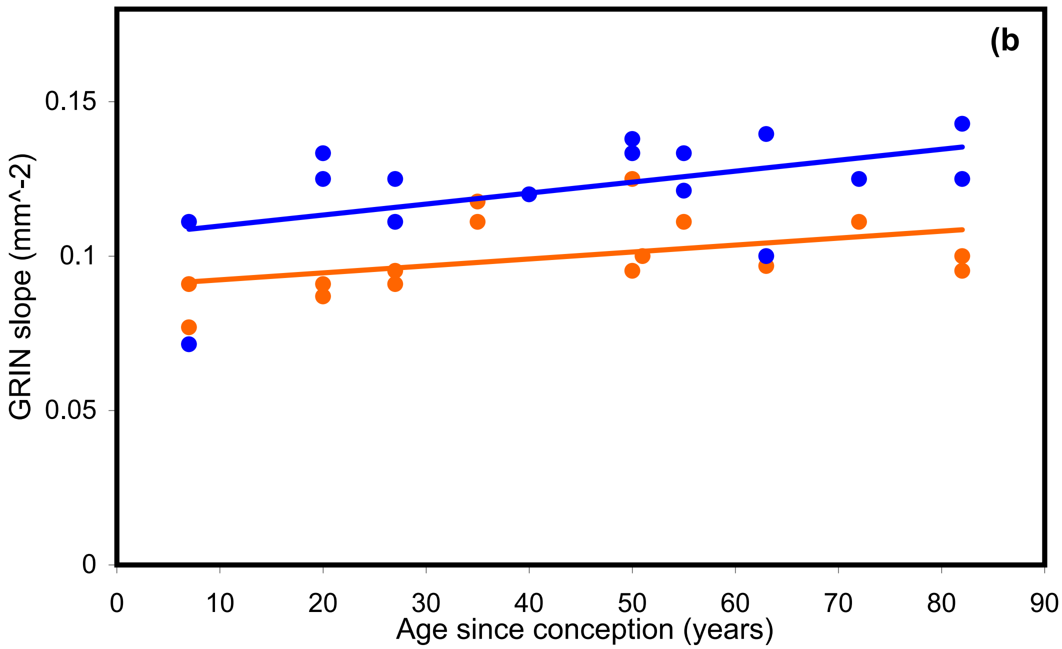
(b
GRIN slope (mm^-2)
0.15
0.1
0.05
0
0
10
20
30
40
50
60
70
80
90
Age since conception (years)

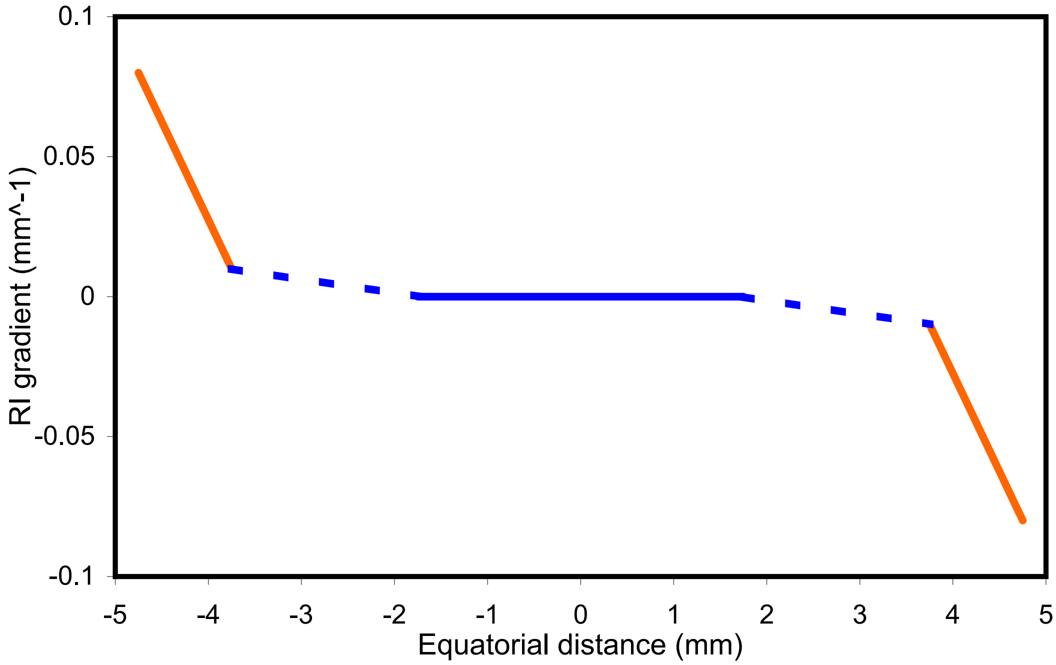
0.1
0.05
0
-0.05
-0.1
RI gradient (mm^-1)
-5
-4
-3
-2
-1
0
1
2
3
4
5
Equatorial distance (mm)

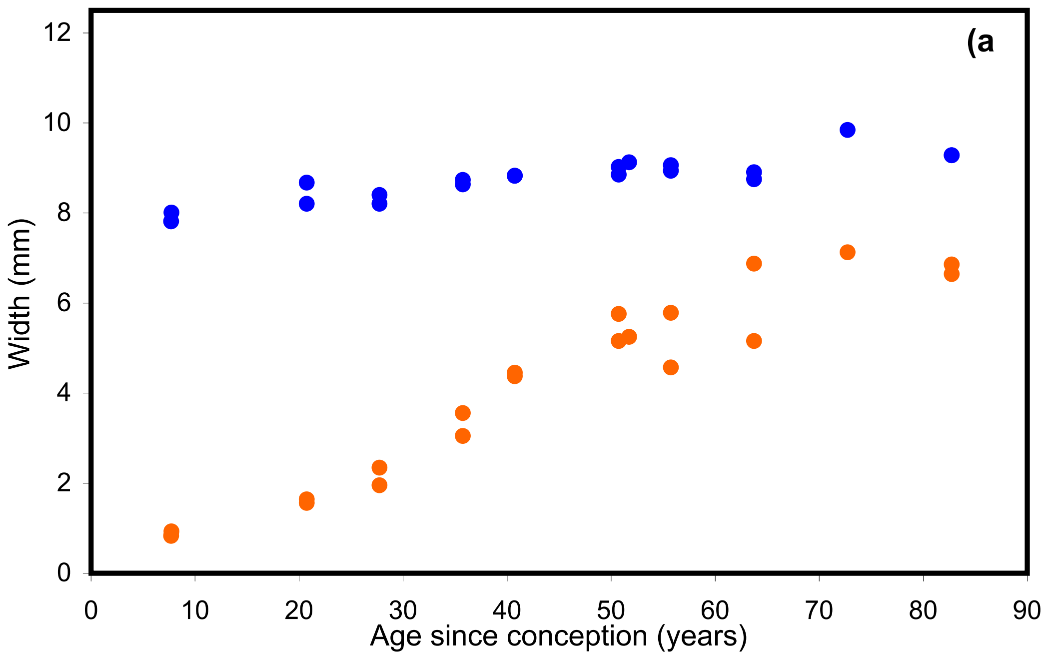
(a
Width (mm)
12
10
8
6
4
2
0
0
10
20
30
40
50
60
70
80
90
Age since conception (years)

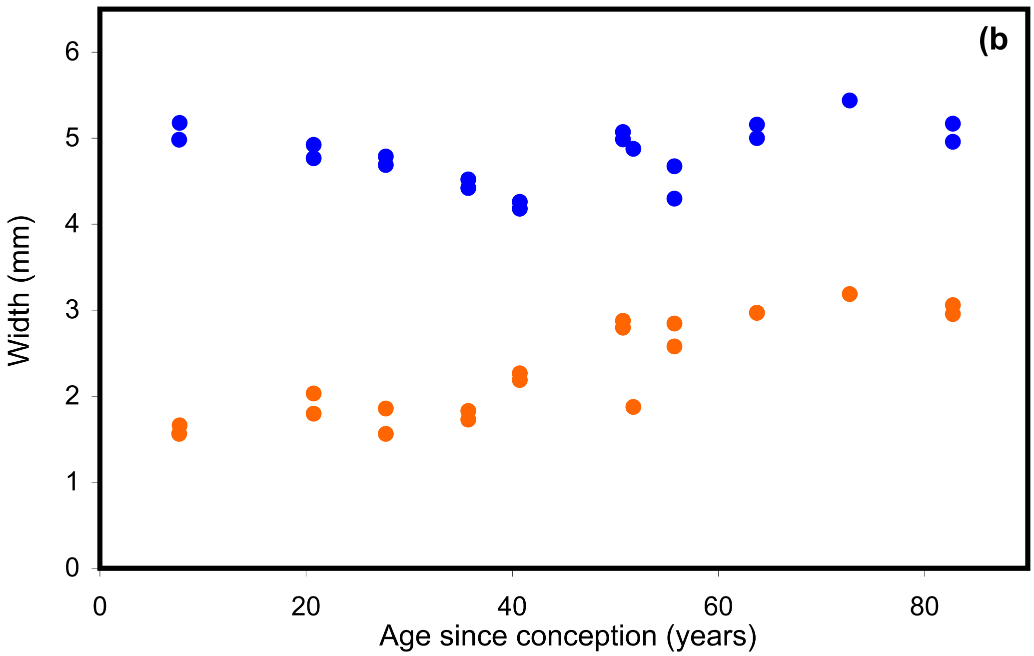
(b
Width (mm)
0
1
2
3
4
5
6
0
20
40
60
80
Age since conception (years)